Surface emitting thermally assisted polaritonic light-emitting device

D. Chastanet, J.-M. Manceau, T. Laurent, A. Bousseksou, G. Beaudoin, I. Sagnes, and R. Colombelli

Citation: Appl. Phys. Lett. **110**, 081108 (2017); doi: 10.1063/1.4976585
View online: http://dx.doi.org/10.1063/1.4976585
View Table of Contents: http://aip.scitation.org/toc/apl/110/8
Published by the American Institute of Physics

Surface emitting thermally assisted polaritonic light-emitting device

D. Chastanet, J.-M. Manceau, T. Laurent, A. Bousseksou, G. Beaudoin, I. Sagnes, and R. Colombelli
Centre de Nanosciences et de Nanotechnologies, CNRS, Univ. Paris-Sud, Université Paris-Saclay, C2N – Orsay, 91405 Orsay cedex, France

(Received 21 November 2016; accepted 29 January 2017; published online 23 February 2017)

We report a mid-infrared surface-emitting electroluminescent device operating in the strong coupling regime between light and matter. The structure is semiconductor based and can operate in absorption or—upon current injection—in emission. The observed minimum Rabi splitting at room-temperature is of the order of 15% of the bare transition. The polaritonic electroluminescence matches the polaritonic branches as measured in absorption and it tunes in frequency with the emission angle, covering a wide spectral range from 900 cm^{-1} to 1300 cm^{-1}. The emitted light is mostly transverse-magnetic polarized, but its intensity increases with increasing temperature. This finding suggests a thermally assisted emission process. A simple model that takes into account both the contributions reproduces the data fairly well. This grating-based, surface-emitting resonator architecture suits the future study and development of electroluminescent intersubband devices operating in the strong-coupling regime between light and matter. *Published by AIP Publishing.*
[http://dx.doi.org/10.1063/1.4976585]

Microcavity instersubband polaritons are mixed states: they are the new eigenmodes that arise when the coupling between the electronic transition and a microcavity photon mode is faster than the damping rates.[1–4] The use of a quantum cascade (QC) approach to achieve photon emission from intersubband (ISB) cavity polaritons has been proposed in the past.[5] It was then implemented in the mid-infrared spectral range[6,7] and also—as a preliminary demonstration—in the THz range.[8] The idea in Ref. 5 and in the following literature was that judicious quantum engineering of the electronic band structure and the microcavity resonator allows one to obtain emission in the strong light–matter coupling regime under electrical excitation. The *initial* perspective was to develop ISB light emitting devices (LEDs) with much higher quantum efficiency than an ISB LED operating in the weak coupling regime. However, it appears that—with the current techniques—when injecting electrons in the system, most of the energy is transferred to dark modes, which do not couple with the electromagnetic field.[9] The resulting quantum efficiencies are low. A possible alternative is to optically pump the polaritonic system to excite *bright* states only,[10] with the perspective of developing ISB polariton lasers.[11]

However, electrical injection is always a powerful asset for an optoelectronic device. Elucidating the mechanism of electronic injection into a polaritonic system is therefore important, with the perspective—in the long term—of circumventing the problem of *dark states*. For instance, in Ref. 7, a signature of the scattering between microcavity polaritons and longitudinal optical phonons was observed in an electroluminescent (EL) device. Such a scattering mechanism is important since it could be *stimulated* by bosonic final-state effects and enable—as discussed in Refs. 10 and 11—a polariton laser.

Polariton-phonon scattering is proportional to the product of the *matter* fraction (Hopfield coefficient) of both the initial and final polaritonic states. An extreme example is that polaritons cannot scatter into a purely photonic state. Since judicious dispersion engineering permits to tailor the Hopfield coefficients, it is a powerful tool to engineer scattering processes and it has been in fact an enabling ingredient behind the demonstration of exciton-polariton lasers.[12,13] We have recently shown in Refs. 14 and 15 that properly patterned metal-insulator-metal (MIM) resonators can mimic the polaritonic dispersion of exciton-polariton systems in the mid-infrared ranges of the electromagnetic spectrum.

These resonators couple radiation from the surface and they have been developed primarily for optical pumping experiments.[10] In this letter, we start exploring their potential as a platform for polaritonic LEDs, since they are surface-emitters and electrical contacts can be implemented in a very straightforward way.

The device architecture—depicted in Fig. 1(a)—relies on a metal-insulator-metal (MIM) geometry with a top metallic grating.[15] The device operates around 2nd-order Bragg diffraction. The advantage of this configuration is that the modal dispersion, that can be easily inferred using angle-resolved reflectivity, is similar to the one that has been a crucial tool behind the demonstration of exciton-polariton lasers.[12] We have demonstrated in Ref. 15 the strong light-matter coupling between such mode and a mid-infrared ISB excitation in a semiconductor quantum well (QW) sandwiched between the two metallic surfaces.

In this work, we have instead inserted an electroluminescent QC structure in the MIM resonator, as schematically shown in Fig. 1(b). The structure can be still probed in reflectivity, but also in electroluminescence if proper contact pads are introduced, as shown in Figs. 1(c) and 1(d), that enable vertical transport across the heterostructure. The quantum design is inspired from the design rules defined in Ref. 5. It consists of 16 repetitions of a QC structure that was grown by MOVPE in the InGaAs/AlInAs material system, for a

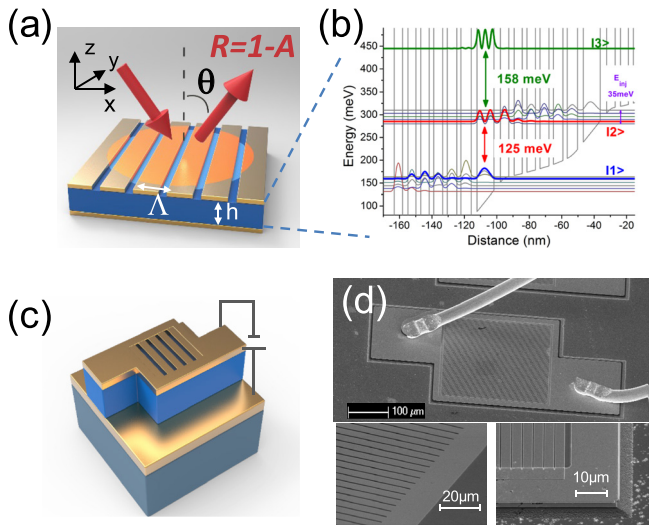

FIG. 1. (a) Schematic of the device processed for reflectivity probing of the strong coupling regime between light and matter. (b) Simulated electronic band-structure of the quantum cascade device used for the electrical excitation of the polariton states. (c) Schematic of the device in the electrical injection configuration. (d) SEM images of a typical processed device.

total thickness h of 1.04 μm. The band diagram of 1.5 periods, calculated with a self-consistent Schrödinger-Poisson solver, is shown in Fig. 1(b). The fundamental radiative transition, between states $|2\rangle$ and $|1\rangle$, takes place in the central QW at a nominal energy of 125 meV (1008 cm^{-1}). Each period of the structure is relatively heavily n-doped to a surface density of 2.31×10^{12} cm^{-2} (see caption of Fig. 1 for details).

The advantage of single-QW based electroluminescent active regions is that they can be tested in absorption too since at zero bias the transition is marginally detuned (no 1st-order Stark effect in single QWs), and electrons are present in the ground state. Figure 2(a) shows the measured transmission at room temperature in a multipass waveguide configuration. A clear transverse-magnetic (TM) polarized absorption is observed at $\nu = 1000\,cm^{-1}$, in agreement with design, with an 8% full-width at half maximum (FWHM).

We have inserted this active region in properly designed grating-based MIM resonators, using the waferbonding techniques thoroughly described in Refs. 15 and 16. Figure 2(b) proves that strong-light matter coupling at room temperature is achieved in this cavity configuration. We probe the reflectivity $R(\omega,\theta)$ over a large bandwidth and over a wide angular range ($13° < \theta < 73°$) using a Fourier transform infrared spectrometer (FTIR) equipped with a Globar thermal source and a deuterated tryglicine sulfate (DTGS) detector. The absolute reflectivity is obtained by normalizing the sample spectrum against a reference obtained on a planar gold surface. The photonic dispersion (ω vs in-plane wavevector) $R(\omega, k_{//})$ is then readily inferred from $R(\omega,\theta)$ using the relationship $k = \frac{\omega}{c}\sin(\theta)$. Upper (UP) and lower (LP) polariton modes clearly appear in the dispersion relation. Note also the presence of the lower *photonic* branch of the cavity that starts at $\sim$900 cm^{-1} and evolves to lower frequencies with increasing k-vector. This branch is invisible at $k = 0$, since it is there rigorously non-radiative,[16] but it becomes more and more evident at large incidence angle as its radiative

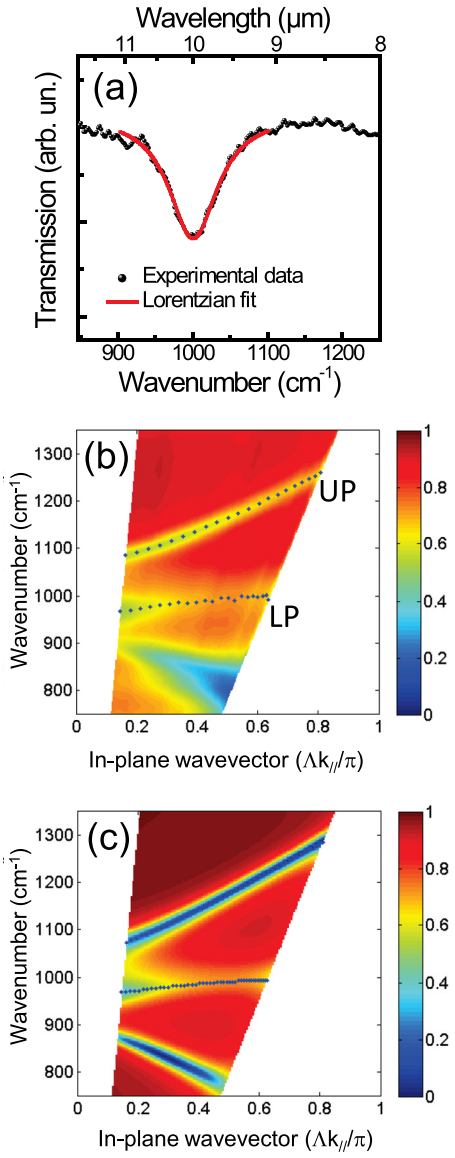

FIG. 2. (a) Measured transmission spectrum of the quantum cascade structure shaped in a multi-pass waveguide configuration. The red dashed curve is the Lorentzian fit to the absorption. (b) Reflectivity measurement of the polaritonic system and (c) RCWA simulation of the same polaritonic system. The grating period is $\Lambda = 3.35$ μm with a filling factor of 80%.

Q-factor (Q_{rad}) decreases. The excellent agreement with RCWA (rigorous coupled-mode theory analysis) simulations, shown in Fig. 2(c), further confirms that the device operates in strong coupling. The RCWA simulations employ the same approach as in Ref. 17. The complex dielectric constant of gold is taken from Ordal,[18] while the ISB transition contribution of the active region is included in the z-component of the dielectric tensor using the Zaluzny-Nalewajko approach.[19]

We now discuss the experimental results in emission, i.e., when current is driven through the QC structure and the emitted light is measured using a Mercury Cadmium Telluride detector cooled at 78 K in combination with the FTIR. A gold coated off-axis parabolic mirror with an f-number of 1 was used to collect the signal. Figure 3 resumes the measurements when the QC structure is operated in weak coupling. To do so, it was processed in a large mesa configuration (200 μm

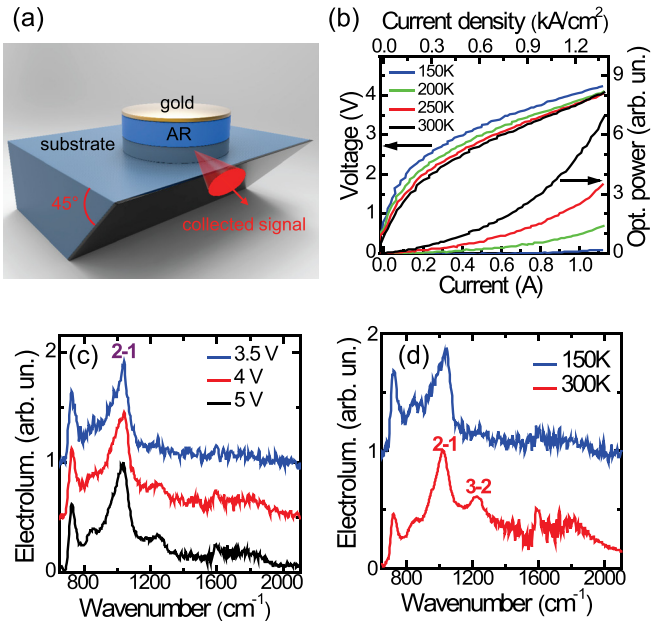

FIG. 3. Opto-electrical characterizations in weak-coupling. (a) Scheme of the device, a 200-μm-diameter mesa. Emitted light is collected from a 45° polished facet. (b) Light-voltage-current (LVI) characteristics for different heat-sink temperatures. (c) Normalized emission spectra measured at 200 K for different applied voltages. (d) Normalized emission spectra measured at 4 V applied voltage on the same device for two different temperatures.

diameter, Fig. 3(a)) with top and bottom contacts, and light was collected from a 45° polished facet. The light-voltage-current (LVI) characteristics in Fig. 3(b) reveal two main peculiarities: the light output is superlinear with current and the overall emitted power *decreases* when lowering the heat-sink temperature down to 150 K. Below that temperature, we are not able to measure any significant amount of signal. The first observation suggests that the light emission is possibly dominated by a thermal component.[20] The second observation is instead related to *Fermi filling* of the active QW fundamental subband.

The sample is designed, following Ref. 5, in order to have a density of electrons N_1 in the fundamental subband much larger than the density N_2 in the excited subband even under an applied bias. The EL signal stems from radiative transitions undergone by electrons from the excited to the fundamental subband. To this scope, *holes* in the fundamental subband must be present, but their number—following the Fermi-Dirac statistics—drops dramatically at low temperature, thus quenching the radiative efficiency.

For the given collection optics (f-number = 1) and without considering the different losses induced by the optics and the spectrometer path, we collect approximately 15 nW of optical power at 150 K and 990 nW at 300 K, for an injected electrical power of 500 mW. The respective efficiencies are 3×10^{-8} at 150 K and 2×10^{-6} at 300 K.

The aforementioned interpretation is corroborated by the spectral measurements at variable applied voltages and heat-sink temperature. Figure 3(c) shows normalized EL spectra measured at 200 K for different voltages. At 3.5 V, the main emission peak at 1000 cm^{-1} stems from the ISB transition (the low energy peak at ~750 cm^{-1} is possibly a convolution between plasma emission from the n^+-doped contacts and the detector cut-off). Increasing the applied voltage leads to the emergence of a broad background, which we identify as a thermally assisted emission process and explains the superlinear dependence of the LI curve in Fig. 3(b). A similar confirmation can be inferred from Figure 3(d), which reports instead normalized EL spectra for two different temperatures (150 K and 300 K), with 4 V bias applied on the device.

When the QC active region is processed into the grating-based, electrically compatible resonators depicted in Figs. 1(c) and 1(d), the device operates as an LED operating in the strong coupling regime between light and matter. Figure 4(a) shows the experimental data: the measured electroluminescence dispersion acquired at a temperature of 150 K. We measure the spectrally and angularly resolved sample electroluminescence EL(ω,θ) over a large bandwidth and over a wide angular range. Note: in this emission configuration, we overcome the angular limitation of the passive probing and we can record the dispersion down to k = 0. The dispersion relation in emission EL(ω,k) is then readily obtained from EL(ω,θ). The excellent agreement between the emission data (color plot) and the reflectivity data (open dots) permits to unambiguously assign the emission peaks to the polaritonic states of the system. As for the emitted power,

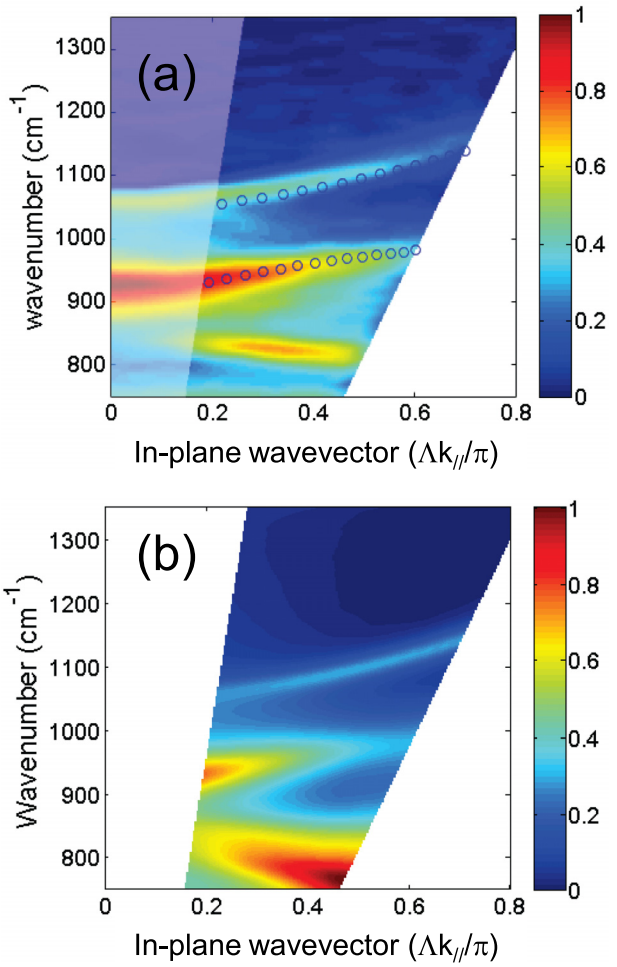

FIG. 4. (a) Experimental polaritonic dispersion obtained from angle-resolved electroluminescence measurements at 150 K for an applied voltage of 4.1 V. The sample features a top grating with period L = 3.75 μm and filling factor 80%. The open dots mark the position of UP and LP as obtained from the reflectivity measurements. (b) Calculated polaritonic dispersion. It is obtained as the product between the absorbance (1-R(ω, $k_{//}$)) and the spectral emissivity of an ideal blackbody at a temperature of 300 K.

we find that the efficiency of the strongly coupled system is similar to the one of the weakly coupled system: in the 10^{-6} range at room temperature and in the 10^{-8} range at 150 K. There is no evidence, at this stage, of any emission enhancement due to operation in the strong-coupling regime. The question is *how* the polaritonic states are excited: through a direct electronic injection into polariton states, as discussed for instance in Ref. 9, or via the excitation of a broadband/thermal source inside the cavity?

To elucidate this point, we have simulated the experimental electroluminescence as the product of the experimental absorption (1-R(ω, $k_{//}$)) *times* the spectral emissivity of a blackbody at temperature T, $E_{BB}(\nu,T)$, following Planck's law:

$$E_{BB}(\nu, \mathrm{T}) = \frac{2h\nu^3}{c^2}\frac{1}{e^{\frac{h\nu}{k_B T}} - 1},$$

where k_B is the Boltzmann constant. The result of the simulation is shown in Fig. 4(b) and it is in excellent agreement with the experimental data. This finding suggests that, although the emission peak at $\nu = 1000\,\mathrm{cm}^{-1}$ in weak coupling stems from the ISB 2→1 transition inside the QC active region, the overall electroluminescent behavior of the device in strong coupling originates from a thermally assisted emission process. It also suggests, as expected, that the "effective" temperature of the active region under electrical pumping is higher than the heat-sink. We find in fact a good agreement between experiment and theory when using a blackbody temperature of 300 K.

Does this experiment absolutely exclude that we are injecting energy into the polaritonic system, and we are instead just *heating* the device, albeit operating it in the strong-coupling regime? This is a complex issue that has been discussed in a series of theoretical papers,[9,21] but—to date—was never elucidated experimentally. We believe that the grating-based, dispersive resonators presented in this work are a promising tool to study this topic, since they have several advantages. Namely, electrical injection is extremely easy, as well as the experimental analysis of the polaritonic dispersion *via* simple angle-resolved measurements on a single device. Furthermore, it is possible - up to a certain extent - to engineer the Hopfield coefficients of the system. The limit of the current experiment is that the device EL in *weak-coupling* is broadband, and its width is larger than the experimental polaritonic splitting. This makes difficult to discriminate from true injection into the polaritonic system, and a thermally assisted process. The solution, that is also the next step, is to employ a QC structure that exhibits an EL in weak-coupling that is *narrower* than the polaritonic splitting.

The only suggestive observation that we can make on the current system is based on the comparison of the polaritonic dispersion in emission at two different temperatures, 300 K and 150 K, as reported in Fig. 5. The polaritonic features narrow, as expected when lowering the temperature. However, the extension in k-space of the UP and LP increases at low temperature. The vertical white dashed line marks the $k_{//} = 0.2$ position: the UP has a signal of 0.6 here at 300 K, while at 150 K it is still more than 0.8 (the EL is normalized in the two plots), and a signal as low as 0.6 is reached only at $k_{//} = 0.4$. This cannot be explained in a purely thermal model and might suggest that temperature-dependent scattering mechanisms (phonon-polariton; polariton-polariton) could be at play. Note that instead the purely photonic branch (around 900 cm^{-1}, surrounded in a dashed black line) does not undergo the same phenomenon.

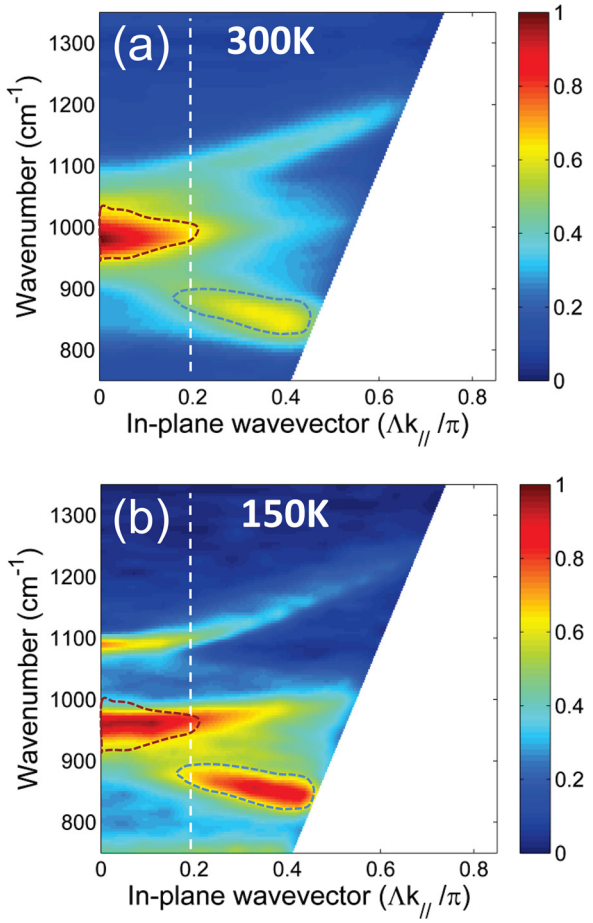

FIG. 5. (a) Measured electroluminescence dispersion at 300 K. (b) Measured electroluminescence dispersion at 150 K. Both are obtained with the same device having a period of L = 3.35 μm and a filling factor of 80% and for an applied voltage of 4.1 V. The plots are normalized to the maximum EL signal at $k_{//} = 0$, which is the peak emission of the lower polariton branch. The vertical white dashed line marks the $k_{//} = 0.2$ position. The dashed black lines circle regions of equal area in the two plots.

In conclusion, we have reported a mid-infrared surface-emitting electroluminescent device operating in the strong coupling regime between light and matter. The polaritonic emission covers a wide spectral range from 900 cm^{-1} to 1300 cm^{-1}, and the minimum Rabi splitting is of the order of 15% at room temperature. The emitted light is mostly transverse-magnetic polarized, but its intensity increases with increasing temperature, suggesting a thermally assisted emission process. We do not have evidence of emission enhancement when operating the device in the strong-coupling regime, an observation that corroborates the thermally excited character of the system. The next generation of device will employ the same grating-based, surface-emitting architecture that we find quite powerful, in combination with a narrowband intersubband emitter. This will permit to study experimentally the details of the electronic injection into the polaritonic states.

We thank F. Julien, A. Vasanelli, and C. Sirtori for useful discussions, and S. Zanotto for the original RCWA code. This work was partly supported by the French RENATECH network. R.C. and T. L. acknowledge support from the ERC "GEM" grant (Grant Agreement No. 306661).

[1]D. Dini, R. Köhler, A. Tredicucci, G. Biasiol, and L. Sorba, Phys. Rev. Lett. **90**, 116401 (2003).
[2]D. Dietze, a. M. Andrews, P. Klang, G. Strasser, K. Unterrainer, and J. Darmo, Appl. Phys. Lett. **103**, 2011 (2013).
[3]A. Benz, S. Campione, M. W. Moseley, J. J. Wierer, A. A. Allerman, J. R. Wendt, and I. Brener, ACS Photonics **1**, 906 (2014).
[4]J. Lee, S. Jung, P.-Y. Chen, F. Lu, F. Demmerle, G. Boehm, M.-C. Amann, A. Alù, and M. A. Belkin, Adv. Opt. Mater. **2**, 1057 (2014).
[5]R. Colombelli, C. Ciuti, Y. Chassagneux, and C. Sirtori, Semicond. Sci. Technol. **20**, 985 (2005).
[6]L. Sapienza, A. Vasanelli, R. Colombelli, C. Ciuti, Y. Chassagneux, C. Manquest, U. Gennser, and C. Sirtori, Phys. Rev. Lett. **100**, 136806 (2008).
[7]A. Delteil, A. Vasanelli, P. Jouy, D. Barate, J. C. Moreno, R. Teissier, A. N. Baranov, and C. Sirtori, Phys. Rev. B **83**, 81404 (2011).
[8]M. Geiser, G. Scalari, F. Castellano, M. Beck, and J. Faist, Appl. Phys. Lett. **101**, 141118 (2012).
[9]S. De Liberato and C. Ciuti, Phys. Rev. B: Condens. Matter Mater. Phys. **79**, 075317 (2009).
[10]R. Colombelli and J.-M. Manceau, Phys. Rev. X **5**, 011031 (2015).
[11]S. De Liberato and C. Ciuti, Phys. Rev. Lett. **102**, 136403 (2009).
[12]D. Bajoni, J. Phys. D: Appl. Phys. **45**, 313001 (2012).
[13]A. Imamoglu, R. Ram, S. Pau, and Y. Yamamoto, Phys. Rev. A **53**, 4250 (1996).
[14]J. M. Manceau, S. Zanotto, I. Sagnes, G. Beaudoin, and R. Colombelli, Appl. Phys. Lett. **103**, 091110 (2013).
[15]J.-M. Manceau, S. Zanotto, T. Ongarello, L. Sorba, A. Tredicucci, G. Biasiol, and R. Colombelli, Appl. Phys. Lett. **105**, 81105 (2014).
[16]G. Xu, R. Colombelli, S. P. Khanna, A. Belarouci, X. Letartre, L. Li, E. H. Linfield, A. G. Davies, H. E. Beere, and D. A. Ritchie, Nat. Commun. **3**, 952 (2012).
[17]S. Zanotto, G. Biasiol, R. Degl'Innocenti, L. Sorba, and A. Tredicucci, Appl. Phys. Lett. **97**, 231123 (2010).
[18]M. A. Ordal, L. L. Long, R. J. Bell, S. E. Bell, R. R. Bell, R. W. Alexander, and C. A. Ward, Appl. Opt. **22**, 1099 (1983).
[19]M. Załużny and C. Nalewajko, Phys. Rev. B **59**, 13043 (1999).
[20]T. Laurent, Y. Todorov, A. Vasanelli, I. Sagnes, G. Beaudoin, and C. Sirtori, Appl. Phys. Lett. **107**, 241112 (2015).
[21]S. De Liberato and C. Ciuti, Phys. Rev. B: Condens. Matter Mater. Phys. **77**, 1 (2008).